Synthesis and Characterization of Poly(isobutylene-*b*-pivalolactone) Diblock and Poly(pivalolactone-*b*-isobutylene-*b*-pivalolactone) Triblock Copolymers†

Younghwan Kwon‡ and Rudolf Faust*

Polymer Science Program, Department of Chemistry, University of Massachusetts Lowell, One University Ave., Lowell, Massachusetts 01854

Cinti X. Chen and Edwin L. Thomas

Department of Materials Science and Engineering, Massachusetts Institute of Technology, Cambridge, Massachusetts 02139

Received October 4, 2001; Revised Manuscript Received February 15, 2002

ABSTRACT: The synthesis of poly(isobutylene-*b*-pivalolactone) block copolymers comprised of amorphous rubbery/crystalline block segments was accomplished by site transformation from living cationic polymerization of isobutylene (IB) to anionic ring-opening polymerization (AROP) of pivalolactone (PVL). First, polyisobutylene (PIB) with ω-carboxylate potassium salt was prepared by capping living PIB with 1,1-diphenylethylene followed by quenching with 1-methoxy-1-trimethylsiloxypropene and hydrolysis of ω-methoxycarbonyl end groups. The resulting PIB ω-carboxylate potassium salt was successfully used as a macroinitiator for the AROP of PVL in conjunction with 18-crown-6 in tetrahydrofuran, giving poly(IB-*b*-PVL) copolymers. Furthermore, the same methodology was applied toward poly(PVL-*b*-IB-*b*-PVL) copolymers using PIB α,ω-carboxylate potassium salt as a difunctional macroinitiator. Characterization of the block copolymers by high-temperature GPC, ^{1}H and ^{13}C NMR spectroscopies, DSC, AFM, and polarized optical microscopy confirmed that the block copolymers were comprised of microphase-separated low glass transition amorphous rubbery PIB and high melting crystalline PPVL block segments with predetermined composition and high structural integrity. Comparison of DSC results with morphological studies using AFM and POM indicated that crystallization of PPVL was constrained to the cylindrical and spherical microdomains preexisting in the melt for certain di- and triblock samples.

Introduction

Recent interest in the design and synthesis of block copolymers has been focused on materials with a combination of unique compositional and architectural properties, especially when hydrophobic/hydrophilic,[1] amorphous/crystalline,[2] dendritic/linear,[3] or heteroarms star[4] blocks are combined. This is principally due to recent advances in living polymerization techniques, which allow the precise control of the architecture, molecular weight, and molecular weight distribution of each block segment. Therefore, most block copolymer synthesis has utilized living polymerization systems including anionic, cationic, radical, group transfer, etc., polymerization.

Living cationic sequential block copolymerization has been shown to be a simple and powerful technique for the synthesis of AB type diblock copolymers and ABA type triblock copolymer thermoplastic elastomers (TPEs) composed of an amorphous rubbery polyisobutylene (PIB) segment as the middle block and different amorphous glassy segments as end blocks.[5] Block copolymers containing crystallizable blocks have been studied as alternative TPEs with improved properties and also as novel nanostructured materials with much more intricate microstructures compared to those comprising of all amorphous blocks.[6] Since the interplay of crystallization and microphase segregation of crystalline/amorphous block copolymers greatly influences the final equilibrium ordered states and results in a diverse morphological complexity, there has been a continued high level of interest in the synthesis and characterization of these materials. Because of the lack of suitable vinyl monomers that give rise to a crystallizable segment by cationic polymerization, living cationic sequential block copolymerization is unsuitable for the combination of amorphous/crystalline block segments.

The site transformation technique provides a useful alternative for the synthesis of block copolymers consisting of two monomers that are polymerized only by two different mechanisms. In this method, the propagating active center is transformed to a different kind of active center, and a second monomer is subsequently polymerized by a mechanism different from the preceding one. The key process in this method is the precocious control of α- or ω-end functionality, capable of initiating the second monomer. Although site transformation has been utilized extensively for the synthesis of block copolymers, only a few PIB/crystalline block copolymers, such as poly(L-lactide-*b*-IB-*b*-L-lactide)[7] and poly(ϵ-caprolactone-*b*-IB-*b*-ϵ-caprolactone)[8] copolymers with relatively short PIB block segment ($M_n \leq 10\,000$ g/mol) were reported. This is most likely due to difficulty in quantitative end functionalization of high molecular weight PIB.

We have already reported that ω-end functionalized PIBs can be readily prepared by the intermediate capping reaction of living PIB with non-(homo)polymerizable monomers such as 1,1-diphenylethylene (DPE) and its derivatives, followed by the addition of suitable nucleophiles. Using this methodology, chain-end func-

† Part VII in Polyisobutylene Based Block Copolymers.

‡ Current address: Department of Chemical Engineering, MIT, Cambridge, MA 02139.

10.1021/ma011739b CCC: $22.00
Published on Web 03/27/2002

tional PIBs with a variety of end groups including methoxy, amine, carbonyl, ester, and carboxylate have been prepared.[9−12] It occurred to us that the PIB−carboxylate anion could initiate anionic ring-opening polymerization (AROP) of β-lactones in general, and pivalolactone (PVL) in particular, giving rise to a high melting and highly crystalline block segment. Although the preparation of poly(IB-*g*-PVL) copolymer has appeared,[13] the structural uniformity of this graft copolymer was less satisfactory, which was attributed to uneven distribution of initiating sites on the PIB backbone.

On the basis of recent results on AROP of PVL,[14−17] it is now generally accepted that alkali metal carboxylates initiate the living AROP of PVL that proceeds exclusively on carboxylate propagating species. More importantly, transesterification is absent because carboxylate active species are not nucleophilic enough to initiate intra- and intermolecular backbiting reactions. PIB having ω-carboxylate functional group can be readily prepared by the hydrolysis of ω-methoxycarbonyl functionalized PIB, obtained by the intermediate capping of living PIB with DPE, followed by end-quenching with silyl ketene acetals.[18] It was found that the methoxycarbonyl end arising by quenching with 1-methoxy-1-trimethylsiloxy-2-methylpropene could not be hydrolyzed under either basic or acidic conditions. The sterically less hindered esters, however, readily underwent hydrolysis. Therefore, the sterically less hindered monomethyl-substituted or unsubstituted silyl ketene acetal derivatives are necessary to obtain ω-carboxylate functional PIB that could initiate the AROP of PVL.

In this article results on the synthesis and characterization of novel AB and ABA type block copolymers consisting of amorphous rubbery PIB (B) segment and high melting crystalline PVL (A) segment via transformation from living cationic to AROP are presented. The crystallization and morphological behavior of these crystalline/amorphous block copolymers was also investigated using DSC, AFM, and polarized optical hot stage microscopy.

Experimental Section

Materials. PVL was prepared by reaction of 3-chloropivalic acid (Aldrich, 99%) with sodium hydroxide according to the procedure described by Lorenz[19] and distilled under reduced pressure. PVL was additionally dried over calcium hydride (CaH_2) for 48 h and distilled under reduced pressure just prior to use. Tetrahydrofuran (THF) was first refluxed over CaH_2 for 48 h and distilled. Subsequently, it was refluxed over the Na/benzophenone complex for 48 h and distilled just before use. Potassium acetate (Aldrich) was dried for 48 h at 40 °C under vacuum. 18-Crown-6 (Aldrich) was dried for 60 h at 50 °C under vacuum. 1-Methoxy-1-trimethylsiloxypropene (MTSP) was synthesized according to Anisworth et al.[20] The synthesis of 2-chloro-2,4,4-trimethylpentane (TMPCl) and 5-*tert*-butyl-1,3-bis(1-chloro-1-methylethyl)benzene (*t*-BuDiCumCl) has been described.[21,22] All other chemicals and solvents were purified as described previously[23,24] or used as received.

Synthesis of Polyisobutylene (PIB) Macroinitiators Carrying ω- or α,ω-Carboxylate Functional Group. For the synthesis of ω-carboxylate PIB macroinitiator, the living cationic polymerization of IB was first carried out at −80 °C in a hexane (Hex)/methyl chloride (MeCl) (60/40 v/v) solvent mixture using the following typical concentrations of reactants: [TMPCl] = 2.0×10^{-3} M, [IB] = 7.1×10^{-2} M, [$TiCl_4$] = 3.6×10^{-2} M, and [2,6-di-*tert*-butylpyridine, DTBP] = 3.0×10^{-3} M. Only the concentration of IB was changed for obtaining the desired molecular weight of PIB segment. After complete monomer conversion (1 h reaction time), the capping reaction of living PIB was accomplished by adding 2 equiv of DPE stock solution. For subsequent in-situ chain-end functionalization, after 1 h capping time 2 equiv of MTSP stock solution was added into the above reaction mixture. After 1 h reaction time, the reaction mixture was quenched with prechilled methanol and poured in NH_4OH/methanol (10/90 v/v) to neutralize the reaction mixture. The obtained polymer was purified by repeated precipitation from Hex into methanol, followed by drying in a vacuum.

The ω-carboxylate potassium salt of PIB was obtained by the hydrolysis of methyl ester group of the above polymer: Into the reactor containing a stirred solution of polymer (0.5 g, $\bar{M}_n$ = 1920 g/mol, $\bar{M}_w/\bar{M}_n$ = 1.06) in 5 mL of toluene, 20 mL of saturated solution of KOH (8.3%, w/v) in hexanol/water (98/2 v/v) was added. The solution was maintained at 100 °C for 24 h and precipitated into methanol. The precipitated polymer was filtered and purified by repeated dissolution/precipitation in Hex/methanol.

For the synthesis of α,ω-telechelic PIB macroinitiator, the living cationic polymerization of IB was carried out at −80 °C in Hex/MeCl(60/40 v/v) using the following typical concentrations of reactants: [*t*-BuDiCumCl] = 1.0×10^{-3} M, [$TiCl_4$] = 3.6×10^{-2} M, and [DTBP] = 3.0×10^{-3} M. The chain-end functionalization of living PIB was achieved by adding 2 equiv of DPE, followed by the addition of 2 equiv of MTSP, as described for the synthesis of ω-carboxylate PIB macroinitiator. Finally, the hydrolysis of methyl ester group of the obtained polymer resulted in the α,ω-carboxylate potassium salt of PIB: The polymer obtained above (4 g, $\bar{M}_n$ = 41 300 g/mol, $\bar{M}_w/\bar{M}_n$= 1.07) was dissolved in 70 mL of toluene. A 56 mL aliquot of saturated solution of KOH (8.3%, w/v) in hexanol/water (98/2 v/v) was added to the solution, and after hydrolysis at 100 °C for 24 h the solution was precipitated into methanol. The precipitated polymer was filtered and purified by repeated dissolution/precipitation in Hex/methanol.

Anionic Ring-Opening Polymerization of PVL. The polymerization of PVL was conducted in a MBraun stainless steel glovebox under a dry nitrogen atmosphere at 25 °C. Into the reactor containing the previously prepared ω-carboxylate or α,ω-carboxylate PIB macroinitiator, THF, and 18-crown-6, the required amount of PVL was added. After a specified period of time, the obtained polymer was precipitated in acidic methanol or Hex. Then the polymer was washed, recovered by filtration, and dried under vacuum. For comparison, PPVL was also polymerized using potassium acetate initiator at room temperature or 70 °C in THF. The polymer, a fine white powder, was washed and extracted with methylene chloride and finally dried under vacuum at 50 °C.

Characterization. ^1H and ^{13}C NMR spectra were measured by using a Bruker 250 MHz instrument in deuterated chloroform ($CDCl_3$) for original PIB and PIB macroinitiators and in a 95/5 (v/v) mixture of $CDCl_3$ and trifluoroacetic acid (TFA) for PPVL and block copolymers.[25] The number-average molecular weight ($\bar{M}_n$) of the PPVL segment in block copolymers was estimated by ^1H NMR spectroscopy from the intensity ratio of the PIB methylene group signal at δ = 1.47 ppm and the signal of the PPVL methylene group at δ = 4.10 ppm.

Molecular weights and molecular weight distributions of the original PIB and ω-methoxycarbonyl functionalized PIB were measured at room temperature using GPC (gel permeation chromatography) equipped with a Waters model 510 pump, a Waters model 486 tunable UV/vis detector, a model 250 dual refractometer/viscometer detector (Viscotek), a Waters model 712 sample processor, and five Ultrastyragel GPC columns connected in the following series: 500, 10^3, 10^4, 10^5, and 100 Å. THF was used as the eluent at a flow rate of 1 mL/min.

High-temperature GPC measurements for block copolymers were performed at 135 °C using a Waters 150-C ALC/GPC system. Trichlorobenzene (TCB), stabilized with butylated hydroxytoluene (BHT), was used as a mobile phase, and the flow rate was 0.5 mL/min. A set of three Plgel (Mixed-B, 10 μm) was used. Block copolymers were dissolved in the TCB (0.15% (w/v)) by heating at 160 °C in a shaker oven for 3 h,

followed by filtration with 2 μm stainless steel filter. All samples were analyzed using a standard PIB calibration curve.

Differential scanning calorimetry (DSC) was performed with a 2910 modulated DSC (TA Instruments) using a heating/cooling scan rate of 10 °C/min in the temperature range −120 to 240 °C. A nitrogen flow of ca. 30 mL/min was maintained through the sample holder assemblies during all runs, and the sample size was about 6−10 mg. Each sample was first scanned from −120 to 240 °C, maintained at that temperature for 1 min, and cooled until −120 °C. The melting temperature (T_m) of PPVL block and the glass transition temperature (T_g) of PIB segment were taken as the peak temperature of the melting endotherm and as the onset point of the specific heat jumps, respectively, in the heating scan, while the crystallization temperature (T_c) of PPVL block was taken as the peak temperature of the exotherm in the cooling scan.

Optical characterization of the block copolymers was performed on a Leica DMRXP polarizing microscope equipped with a Wild Leitz MPS46 Photoautomat along with a Linkam LTS 350 hot stage and a Linkam TP92 controller. Films were prepared from an isotropic melt of the bulk samples between two microscope coverslips. The heating rate was 20 °C/min, and the temperature was held at the melting temperature for 5−10 min before cooling started at a rate of 10 °C/min.

The block copolymer samples used for AFM imaging were prepared first by melting and recrystallization in order to eliminate any previous thermal history. The bulk polymer samples placed on microglass slides were heated to 260 °C on the hot plate, and a melt was formed. The melt was sheared several times by covering a hot microglass slide on the top and moving it along one direction. The cover slide was removed, and the melt was rapidly cooled by dipping it into liquid nitrogen. The imaging was performed immediately after the film was formed. The sample morphology was imaged with a scanning probe microscope (Digital Instruments Nanoscope III) in tapping mode. Silicon cantilevers oscillating at a frequency in the range of 50−90 kHz were used.

Results and Discussion

Synthesis of PIB ω-Carboxylate Potassium Salt Macroinitiator. The synthetic pathway to PIB ω-carboxylate potassium salt is presented in Scheme 1. The first step is the preparation of PIB with ω-methoxycarbonyl functional group, a precursor for carboxylate group. After the living cationic polymerization of IB using TMPCl/$TiCl_4$/DTBP initiating system in Hex/MeCl (60/40 v/v) at −80 °C, the capping reaction was carried out by reacting living PIB with DPE. Upon addition of DPE to living PIB, a red color slowly developed, indicating a generation of stable diphenylcarbenium ions. Upon addition of MTSP for subsequent chain-end functionalization, the color change from red to dark red appeared immediately. The color disappeared upon quenching with prechilled methanol.

Quantitative ω-methoxycarbonyl functionalization of PIB was indicated by the ^{1}H and ^{13}C NMR spectra of the resulting polymers shown in Figures 1 and 2. To simplify the analysis of functionality by NMR spectroscopy, PIB ($\bar{M}_n$= 1920 and $\bar{M}_w/\bar{M}_n$ = 1.06 by GPC measurement) with and without the functional group at the ω-end were prepared. Assignments of ^{1}H and ^{13}C NMR chemical shifts were based on the spectra of the corresponding model compound (Figures 3 and 4) synthesized by the reaction of TMPCl and DPE, followed by end quenching with MTSP, under similar conditions to that of the ω-methoxycarbonyl functionalized PIB. In Figure 1B characteristic resonance peaks for the original PIBCl (−C**H**$_2$C(C**H**$_3$)$_2$Cl), i.e., the methylene (**c**) and methyl (**d**) protons next to chloro end group at 1.96 and 1.67 ppm, respectively, are clearly absent. New

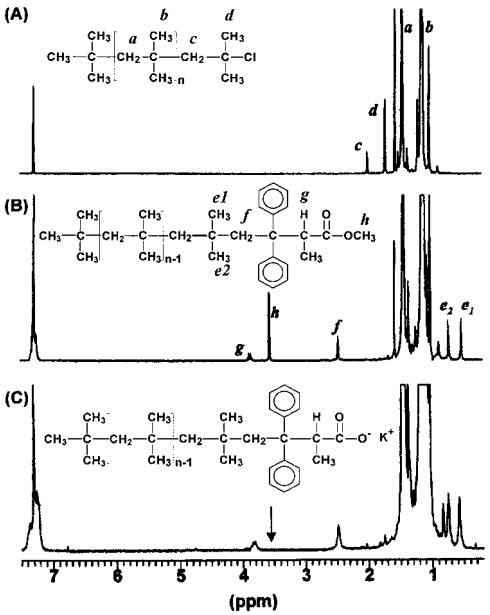

Figure 1. ^{1}H NMR spectra of original polyisobutylene with chlorine end group (PIBCl), ω-methoxycarbonyl functionalized PIB, and ω-carboxylate potassium salt PIB macroinitiator.

Scheme 1. Reaction Scheme for the Synthesis of the ω-Carboxylate Potassium Salt PIB Macroinitiator

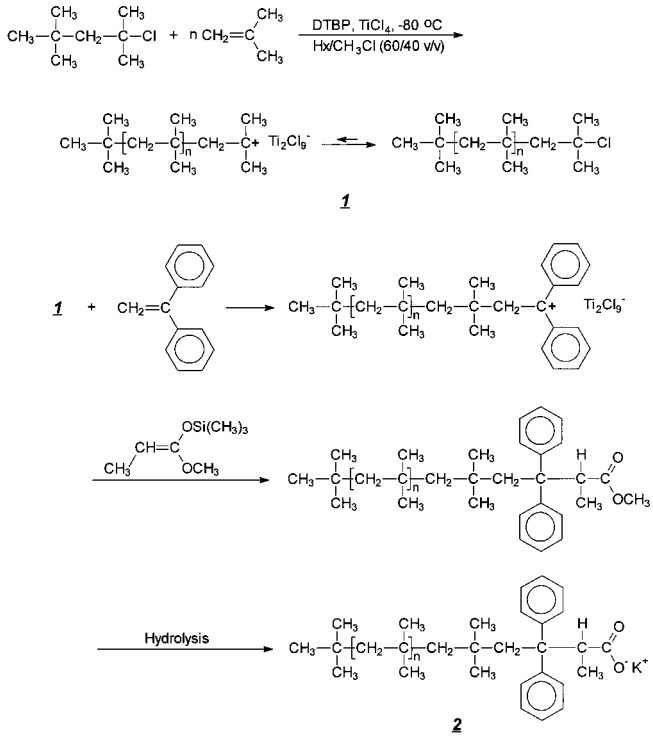

characteristic resonance signals (**e**−**h**) are assigned to ω-methoxycarbonyl functionalized PIB. From the ^{13}C NMR spectrum of the functionalized PIB in Figure 2, it was further confirmed that ω-methoxycarbonyl PIB was obtained. From the signal intensity ratios of peaks (**g** or **h**) to (**e1**, **e2**, or **f**), the number-average end functionality of the polymers was calculated to be very close to unity. In addition, peaks such as PIB-exo olefin (δ = 1.82 (C**H**$_3$), δ = 1.95 (C**H**$_2$), and δ = 4.61 and 4.81 ppm (=C**H**$_2$)), PIB-endo olefin (δ = 5.09 ppm (−C**H**=)), PIB−DPE olefin (δ = 6.20 ppm (−C**H**=)), and PIB−DPE−OCH$_3$ (δ = 2.45 (C**H**$_2$) and δ = 3.00 ppm (−OC**H**$_3$))

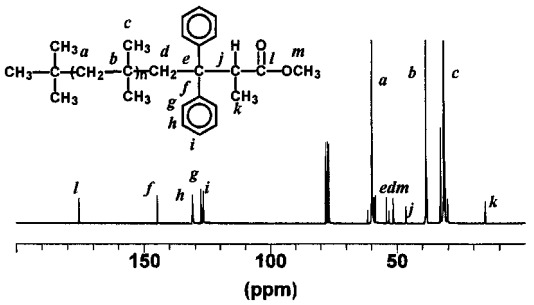

Figure 2. ^{13}C NMR spectrum of ω-methoxycarbonyl functionalized PIB.

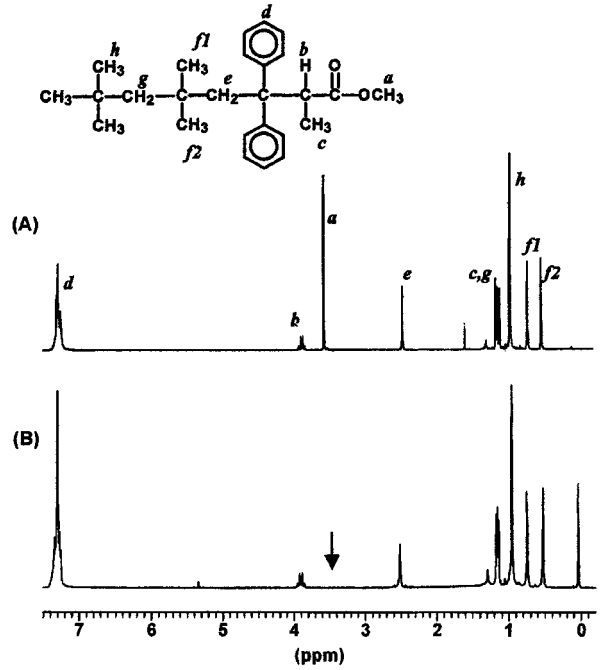

Figure 3. ^{1}H NMR spectra of (A) TMP−DPE−MTSP model compound and (B) after hydrolysis of the model compound.

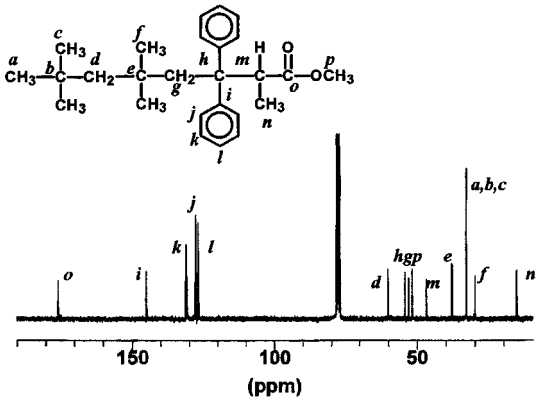

Figure 4. ^{13}C NMR spectrum of TMP−DPE−MTSP model compound.

were virtually absent, strongly confirming quantitative ω-end functionalization as well.

In the second step the methoxycarbonyl groups at the polymer chain ends were quantitatively hydrolyzed into carboxylate groups suitable to initiate AROP of PVL. As shown in Figure 1C, after hydrolysis the characteristic resonance peak at 3.56 ppm corresponding to ω-methoxy protons is completely absent while other peaks remained intact, demonstrating that there was no other change in the polymer structure upon hydrolysis of the ester group.

Scheme 2. Anionic Ring-Opening Polymerization of Pivalolactone Using ω-Carboxylate Potassium Salt PIB Macroinitiator

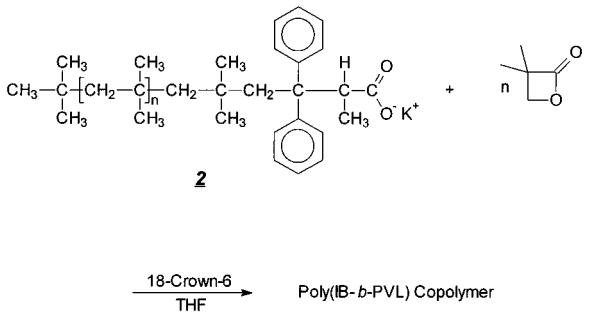

For the subsequent AROP of PVL, the PIB macroinitiator prepared above was purified by repeated dissolution/precipitation from Hex/methanol, respectively, and was dried from anhydrous olefin-free Hex solution.

Synthesis of Poly(isobutylene-*b*-pivalolactone) Copolymers. Scheme 2 shows the block copolymerization of PVL initiated with ω-carboxylate functional PIB macroinitiator, and the results are summarized in Table 1.

In comparison, results of homopolymerization of PVL carried out with potassium acetate initiator in the presence of 18-crown-6 in THF are also shown. The ^{1}H NMR spectrum of PPVL (Figure 5A) shows the signal for the acetoxy ($CH_3C(=O)O-$) headgroup at $\delta = 2.17$ ppm, associated with the initiator residue, and the signals for two methyl ($C\mathbf{H}_3-$) ($\delta = 1.26$ ppm) and one methylene ($-C\mathbf{H}_2-$) ($\delta = 4.20$ ppm) groups in the repeat unit of the polymer. From the ^{1}H NMR spectrum, the number-average molecular weight of PPVL was determined from the signal intensity ratio of the methylene groups in the polymer backbone and the acetoxy end groups, assuming that each polymer chain contains one acetoxy end group. The initiator efficiency was calculated to be ~60%; however, no direct relationship between the molecular weight determined by ^{1}H NMR spectroscopy and the initial monomer-to-initiator ratio was observed. This is presumably due to the heterogeneous nature of the potassium acetate initiator solution in THF, arising from the low solubility of potassium acetate.

As summarized in Table 1, the block polymerization of PVL with PIB macroinitiator proceeds in a desired way to produce poly(IB-*b*-PVL) copolymers in nearly quantitative yield within 6 h. The yield of PVL in the block copolymerization increases with reaction time but decreases with decreasing concentration of PIB macroinitiator. Because of the poor solubility of PPVL blocks in THF, the molecular weight and molecular weight distribution of block copolymers could not be measured by GPC at room temperature. Therefore, the molecular weight of PPVL segment in the block copolymers was calculated from the overall composition determined from the ^{1}H NMR spectrum (Figure 5B) using the integration values of the methylene signals ($\delta = 4.20$ ppm) of PPVL blocks and the methylene signals ($\delta = 1.47$ ppm) of PIB blocks and the molecular weight of the original PIBCl determined by GPC.

By comparison of the ^{1}H and ^{13}C NMR spectra of the block copolymer and homo-PPVL, it is also proved that the block copolymers carry the corresponding signals

Table 1. Results of Anionic Ring-Opening Polymerization of PVL Initiated with Potassium Acetate and ω-Carboxylate Potassium Salt PIB Macroinitiator in Conjunction with 18-Crown-6 in THF

sample	initiator (M)	PVL (M)	temp (°C)	time (h)	yield (%)	$\bar{M}_{n,cald}$[a] of PPVL	$\bar{M}_{n,NMR}$ of PPVL	GPC[f] of block copolymers	
								$\bar{M}_n$	$\bar{M}_w/\bar{M}_n$
D-1	PIB−COOK	1.0	r.t.[e]	4	84.0	2940	2940		
D-2	($\bar{M}_n$ = 2K)[b]	1.0	r.t.	6	∼100	3500	3850		
D-3		1.0	70	6	∼100	3500	3750	3680	1.22
D-4		1.6	70	6	∼100	5400	5660	4810	1.28
D-5	PIB−COOK	0.35	r.t.	6	76.1	4490	4490	21750	1.07
D-6	($\bar{M}_n$ = 20K)[c]	0.70	r.t.	6	∼100	11540	11800	22770	1.08
P-1	AcOK[d]	0.5	70	6	∼ 100	1730	2580		
P-2		1.0	r.t.	6	93.6	3340	5220		

[a] $\bar{M}_{n,cald} = [M]_0/[I]_0 \times$ (yield/100) $\times M$(PVL). [b] $\bar{M}_n$ = 1920; $\bar{M}_w/\bar{M}_n$ = 1.06 (measured by Viscotek); [initiator] = 3.0×10^{-2} M, [18-crown-6] = 3.0×10^{-2} M. [c] $\bar{M}_n$ = 18 000; $\bar{M}_w/\bar{M}_n$ = 1.08 (measured by Viscotek); [initiator] = 5.9×10^{-3} M, [18-crown-6] = 7.0×10^{-3} M. [d] [AcOK] = 3.0×10^{-2} M, [18-crown-6] = 3.0×10^{-2} M. [e] Room temperature, [f] High-temperature GPC.

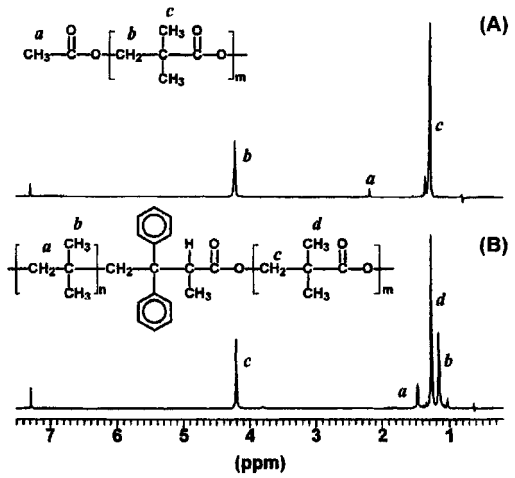

Figure 5. ^{1}H NMR spectra of PPVL (P-1) and poly(IB-*b*-PVL) diblock copolymer (D-4) shown in Table 1.

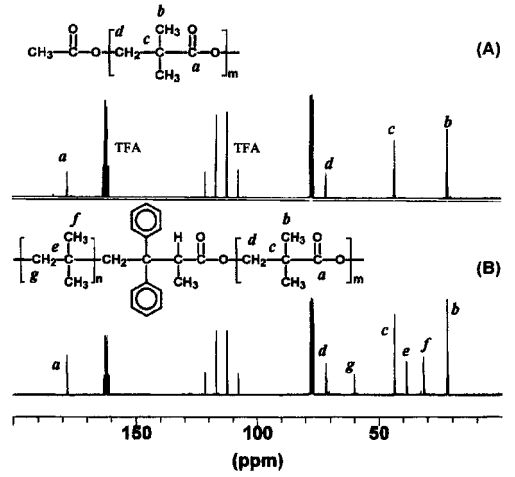

Figure 6. ^{13}C NMR spectra of PPVL (P-1) and poly(IB-*b*-PVL) diblock copolymer (D-4) shown in Table 1.

attributed to the respective characteristic resonance peaks of PIB and PPVL blocks as assigned in Figures 5 and 6. The structural integrity of the poly(IB-*b*-PVL) copolymers obtained was further demonstrated by selective solvent extraction for the block copolymers with PIB ($\bar{M}_n$ = 2K). These unreacted PIBs were easily separated from the block copolymers. The block copolymers synthesized were extracted with Hex, a good solvent for PIB, followed by centrifugation of the suspended solution for 1 h. The upper, clear solution was collected, dried in a vacuum at 50 °C for 24 h, and weighed to

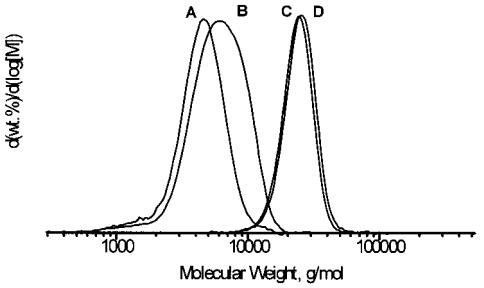

Figure 7. High-temperature GPC traces of poly(IB-*b*-PVL) diblock copolymers: D-3 (A), D-4 (B), D-5 (C), and D-6 (D).

determine the blocking efficiency, which was calculated by following equation

$$\text{blocking efficiency (\%)} = \left(1 - \frac{\text{weight of polymer extracted (g)}}{\text{weight of PIB macroinitiator used (g)}}\right) \times 100$$

From the selective solvent extraction, the blocking efficiency was calculated to be from ∼90 up to ∼96%. The molecular weights calculated from ^{1}H NMR spectroscopy were similar but not identical to those calculated from high-temperature GPC. This is attributed to the relative nature of GPC molecular weights as the determination was based on a calibration curve obtained with PIB standards. More importantly, high-temperature GPC traces shown in Figure 7 of the resulting poly(IB-*b*-PVL) diblock copolymers exhibited monomodal and narrow distributions ($\bar{M}_w/\bar{M}_n$ = 1.07−1.22) shifted to lower elution volume compared to that of the PIB precursor. This suggests that the site transformation technique yields block copolymers with high structural integrity.

From the above results, it can be concluded that the ω-carboxylate PIB macroinitiator with the potassium/18-crown-6 complex counterion efficiently initiates the AROP of PVL that yields poly(IB-*b*-PVL) copolymers of various compositions with high structural integrity.

Synthesis of Poly(pivalolactone-*b*-isobutylene-*b*-pivalolactone) Copolymers. The synthetic procedure for poly(PVL-*b*-IB-*b*-PVL) triblock copolymer is presented in Scheme 3. In the first step, α,ω-methoxycarbonyl functional PIB was prepared by the living cationic polymerization of IB using the *t*-BuDiCumCl/$TiCl_4$ initiating system in the presence of DTBP in Hex/MeCl (60/40 v/v) at −80 °C, followed by capping with DPE and end functionalization with MTSP. Low molecular weight product ($\bar{M}_n$ = 5600 and $\bar{M}_w/\bar{M}_n$ = 1.09 by GPC) was also prepared to simplify the NMR

Scheme 3. Reaction Scheme for the Synthesis of the α,ω-Carboxylate Potassium Salt PIB Macroinitiator

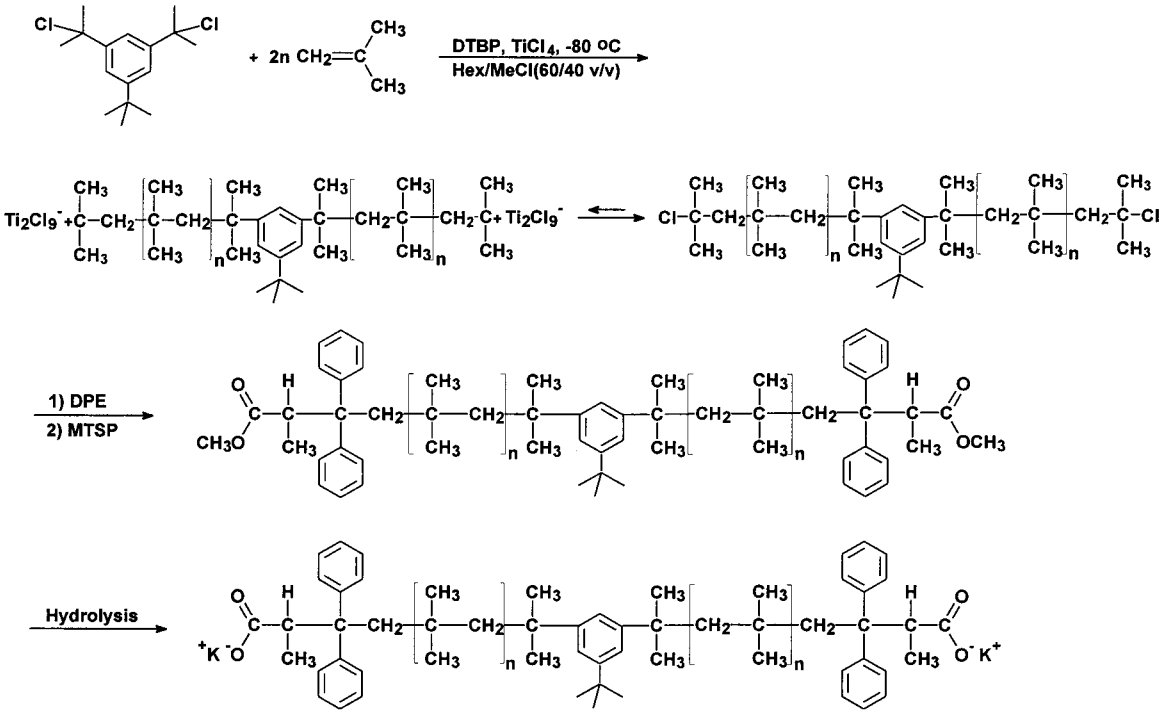

Table 2. Poly(PVL-*b*-IB-*b*-PVL) Triblock Copolymers Synthesized by AROP of PVL Initiated with α,ω-Carboxylate Potassium Salt PIB Macroinitiator[a]

sample		α,ω-carboxylate PIB (M)	PVL (M)	yield (%)	$\bar{M}_{n,NMR}$ of each PPVL block	content of PPVL (wt %)[b]	GPC[e] of block copolymers	
							$\bar{M}_n$	$\bar{M}_w/\bar{M}_n$
T-1	$\bar{M}_n$ = 40K[c]	3.5×10^{-3}	0.70	91.6	9100	31.2	38 100	1.77
T-2		3.5×10^{-3}	0.47	44.6	3200	13.7	42 500	1.23
T-3	$\bar{M}_n$ = 20K[d]	3.5×10^{-3}	0.34	65.8	3500	25.7	24 270	1.10
T-4		3.5×10^{-3}	0.23	42.6	1400	12.4	22 070	1.10

[a] [18-Crown-6] = 3.5×10^{-3} M, THF solvent at room temperature for 18 h. [b] Calculated from ^{1}H NMR comparing integral ratio of methylene peaks of PIB and PPVL. [c] $\bar{M}_n$ = 41 300; $\bar{M}_w/\bar{M}_n$ = 1.07 (measured by Viscotek). [d] $\bar{M}_n$ = 22 100; $\bar{M}_w/\bar{M}_n$ = 1.07 (measured by Viscotek). [e] High-temperature GPC.

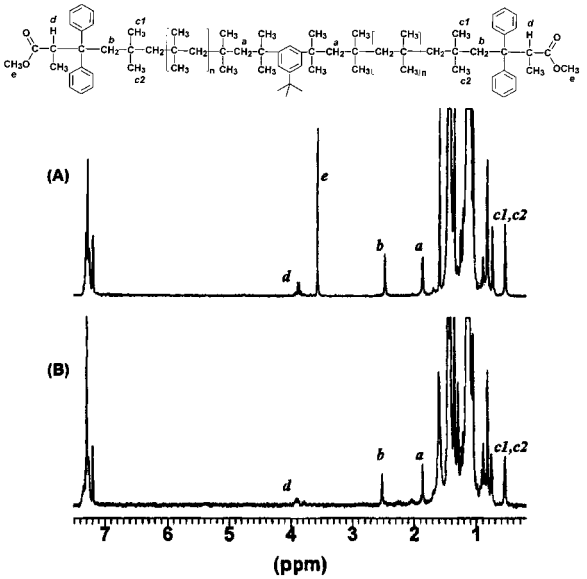

Figure 8. ^{1}H NMR spectra of (A) α,ω-methoxycarbonyl functionalized PIB and (B) α,ω-carboxylate potassium salt PIB macroinitiator.

analysis, and the corresponding ^{1}H NMR spectrum assignment is shown in Figure 8A. In the second step, the hydrolysis of methoxycarbonyl groups at both chain ends in the resulting polymer was carried out by the same method as that for ω-methoxycarbonyl functional PIB. Quantitative hydrolysis was further confirmed by the complete disappearance of peak **e** in the ^{1}H NMR spectrum of the product (Figure 8B).

The α,ω-carboxylate PIB macroinitiator was used for the AROP of PVL in conjunction with 18-crown-6 in THF at room temperature for 18 h to yield the poly(PVL-*b*-IB-*b*-PVL) triblock copolymer. A summary of the results is given in Table 2. Figure 9 shows high-temperature GPC traces of poly(PVL-*b*-IB-*b*-PVL) triblock copolymers synthesized. Except for sample A revealing a small tail/minor peak (<5%) at lower molecular weight, high-temperature GPC traces of the resulting poly(PVL-*b*-IB-*b*-PVL) triblock copolymers demonstrated monomodal and narrow distributions ($\bar{M}_w/\bar{M}_n$ = 1.10−1.23), strongly supporting the synthesis of well-defined triblock copolymers.

DSC thermograms of pristine (unannealed) samples of PPVL homopolymer, poly(IB-*b*-PVL) diblock, and poly(PVL-*b*-IB-*b*-PVL) triblock copolymers are presented in Figure 10. In the heating scan (Figure 10A), the diblock and triblock copolymers exhibited the T_g of amorphous rubbery PIB segment around −71 °C and the T_m of PPVL segment in the range 180−225 °C. This

Table 3. Glass Transition Temperature (T_g), Melting Temperature (T_m), and Crystallization Temperature (T_c) for Block Copolymers Determined from DSC Thermograms

sample	$\bar{M}_{n,total}$[a]	vol fraction (f_{PPVL})[b]	T_g of PIB (°C)	$\bar{M}_{n,PPVL}$[a]	T_m of PPVL (°C)	T_c of PPVL (°C)	% crystallinity ($\Delta H_m/\Delta H_m^0$)	morphology
T-1	58 200	0.27	−67	18200	222	152	65	PPVL cylinders
T-2	46 400	0.11	−66	6400	199	24	72	PPVL spheres
T-3	27 000	0.20	−66	7000	201	146	55	PPVL cylinders
T-4	22 800	0.10	−65	2800	180	119	68	PPVL spheres
D-4	7 660	0.69	N/D[c]	5660	226	168	51	spherulitic
D-5	24 490	0.15	−67	4490	213	31	82	
D-6	31 800	0.31	−67	11800	227	163	70	
P-2	5 220	1.00		5220	220	169	53	spherulitic

[a] Calculated from ^{1}H NMR. [b] Calculated using $d_{PIB} = 0.920$ g/cm^3 and $d_{PPVL} = 1.165$ g/cm^3. [c] Not detected.

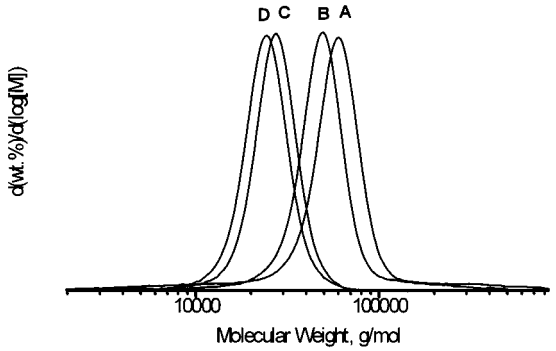

Figure 9. High-temperature GPC traces of poly(PVL-*b*-IB-*b*-PVL) triblock copolymers: T-1 (A), T-2 (B), T-3 (C), and T-4 (D) shown in Table 2.

clearly indicated microphase separation in the block copolymers. Although several data on the T_g of PPVL were reported using relaxation techniques,[26,27] the T_g of PPVL segment was not detected using DSC. To calculate the degree of crystallinity, $\Delta H_m^0 = 148.4$ J/g was taken for 100% crystalline PPVL from the literature.[27] Based on the enthalpy of melting normalized for the content of PPVL in the block copolymers, the degree of crystallinity of PPVL segment in diblock and triblock copolymers was calculated to be in the range 55−82%.

The crystallization behavior of the PPVL segment in the block copolymers is further investigated in the cooling scan of DSC, shown in Figure 10B and summarized in Table 3. The crystallization temperature (T_c) is strongly dependent on the PPVL content, and the observed crystallization temperatures decrease with decreasing volume fraction of PPVL (f_{PPVL}). In the series of diblock copolymers, T_c of sample D-4 ($f_{PPVL} = 0.69$) was detected at a similar temperature to that of PPVL homopolymer (sample P-2), showing T_c at 168 °C. Sample D-6 ($f_{PPVL} = 0.31$) exhibited T_c at 163 °C, i.e., about 5 °C lower than that of PPVL homopolymer; however, T_c of sample D-5 ($f_{PPVL} = 0.15$) decreased to 31.4 °C. A similar observation was also made with triblock copolymers. Above $f_{PPVL} > 0.20$ (samples T-1 and T-3) T_c was in the range 146−152 °C, and at $f_{PPVL} \approx 0.10$ T_c decreased to 119 °C for sample T-4 and fell very abruptly to 24 °C for sample T-2.

When crystallization occurs from a highly segregated block copolymer melt, it is confined to the initial melt morphology.[28,29] Compared to crystallization of a homopolymer, which usually takes place by heterogeneous and/or homogeneous process to form a spherulite, crystallization in a highly segregated block copolymer can only proceed by homogeneous nucleation within the nanoscale domains, which is then the rate-determining step of crystallization.[30] Therefore, crystallization may require large supercooling as seen in DSC results of

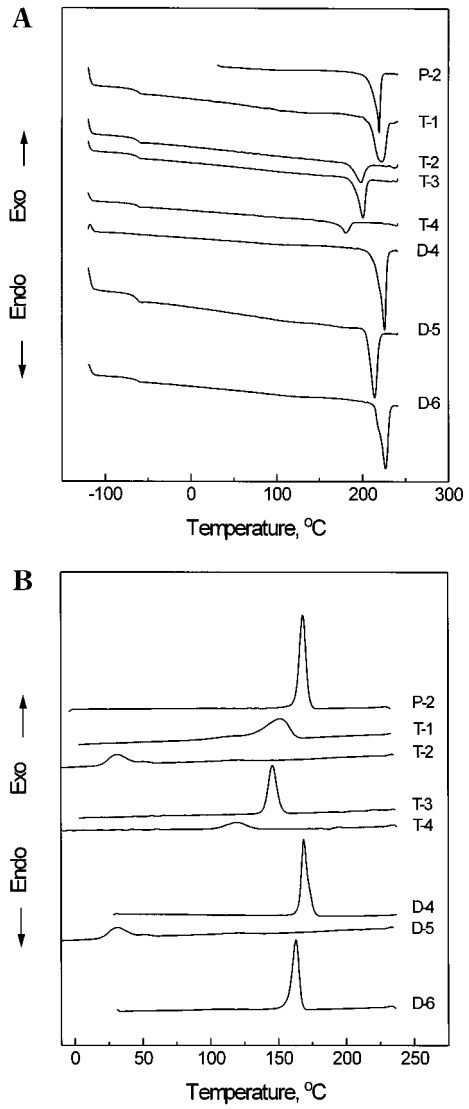

Figure 10. DSC heating (A) and cooling (B) traces at 10 °C/min of PPVL homopolymer, poly(PVL-*b*-IB-*b*-PVL) triblock copolymers, and poly(IB-*b*-PVL) diblock copolymers.

block copolymers with low f_{PPVL}. T_c of samples with lamellar or cylindrical morphology was similar to T_c of homo-PPVL. When the poly(IB-*b*-PVL) and poly(PVL-*b*-IB-*b*-PVL) copolymers exhibited spherical morphology, however, the degree of supercooling for the crystallization in the nanoscale confined domains resulted in drastically reduced T_c, as shown in Figure 11. This observation is somewhat different form the crystallization kinetics reported for PEO−PB diblock-PB homopolymer blends, which showed three distinct regions

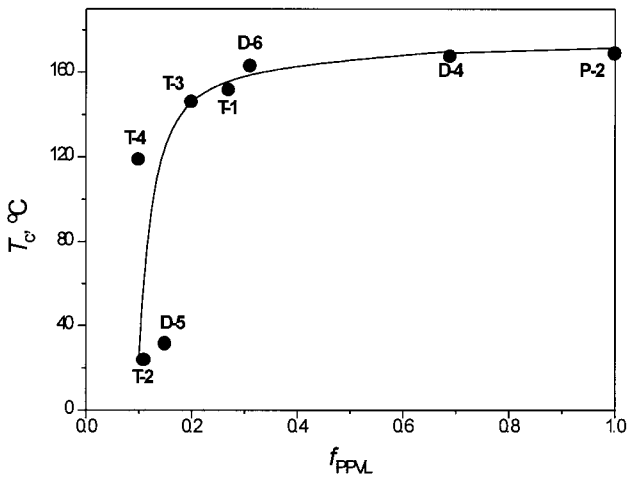

Figure 11. Plot of crystallization temperature (T_c) vs the volume fraction of PPVL (f_{PPVL}) in block copolymers after heating to 240 °C for 1 min and cooling at 10 °C/min.

corresponding to lamellar, cylindrical, and spherical morphologies.[30] This difference might be associated with the characteristics of the crystalline segment, i.e., the rate of crystallization, degree of crystallinity, size of microdomains, etc.

AFM analyses using tapping mode were performed to probe nanoscale morphology of poly(PVL-*b*-IB-*b*-PVL) triblock copolymers in the melt state. Data were recorded using both phase and height imaging, which is appropriate for these block copolymers that have hard (crystalline PPVL) and soft (rubbery PIB) domains. Triblock copolymers with $f_{PPVL} = 0.10$ (sample T-2) show an array of isolated dark spheres in a continuous bright matrix, as shown in Figure 12B. Although bright phase (high phase) in normal tapping mode AFM generally indicates hard segment regions, the phase inversion of hard and soft segments was also reported for poly(styrene-*b*-butadiene-*b*-styrene) (PS−PB−PS) where PS hard domains appeared darker than the PB soft domains at light tapping mode.[31] Since PPVL is the minor component in the block copolymers, the dark region in the phase image can be assigned as spherical domains of PPVL in a continuous PIB matrix phase.

Triblock copolymers with $f_{PPVL} = 0.20$ (sample T-3) and $f_{PPVL} = 0.27$ (sample T-1) are expected to exhibit cylindrical morphologies. Figure 12 (A1) and (A2) are the phase images of sample T-1 melt. Figure 12 (A2) shows arrays of isolated dots, and Figure 12 (A1) shows short cylindrical stripes ordered in one direction. These cylinders may be standing perpendicular to the surface or forming necks emerging to the surface from parallel lying cylinders.[31] The dimensional periodicity (spacing) by SAXS was measured to be 55 nm for T-1, 45 nm for T-2, 30 nm for T-3, and 25 nm for T-4, which are in good agreement with AFM results.

Figure 13 presents optical micrographs of PPVL homopolymer, diblock, and triblock copolymers. PPVL shows the typical spherulite superstructure after crystallization, displaying the characteristic Maltese cross extinction pattern of α-form crystals.[32] Sample D-4 is expected to form a continuous PPVL phase due to the high volume fraction of PPVL ($f_{PPVL} = 0.69$). This sample also exhibits a spherulitic texture indicative of crystallization of PPVL. For diblock copolymers D-5 and D-6, instead of spherulite structures, only a weak birefringence was observed in POM. Similar behavior was observed in triblock copolymers, which all have PPVL

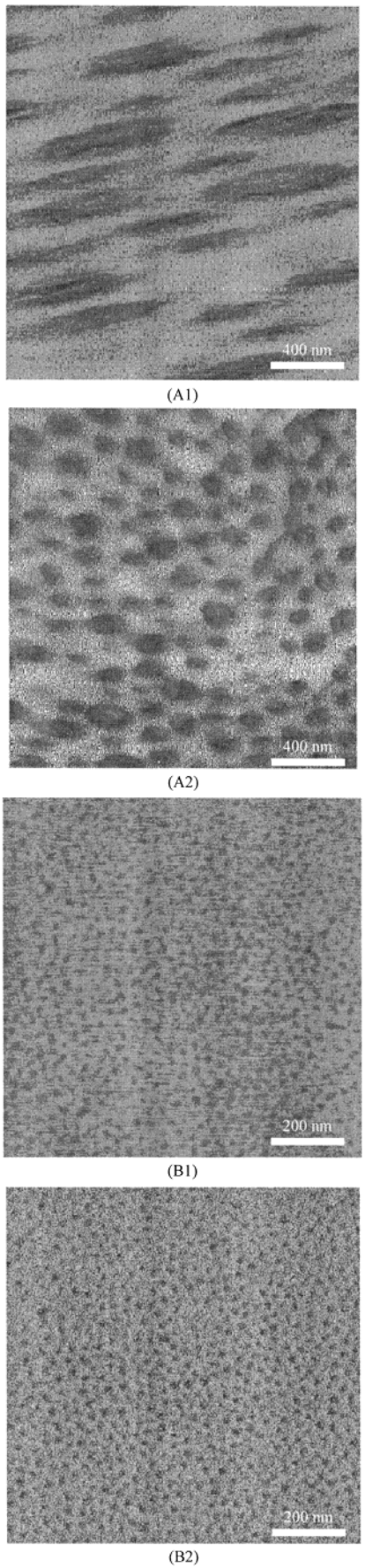

Figure 12. (A1) and (A2) are the phase images of sample T-1: (A1) top view image of the cylindrical direction; (A2) side view image along the cylindrical axis. (B1) and (B2) are from sample T-2: (B1) is the height image; (B2) is the phase image.

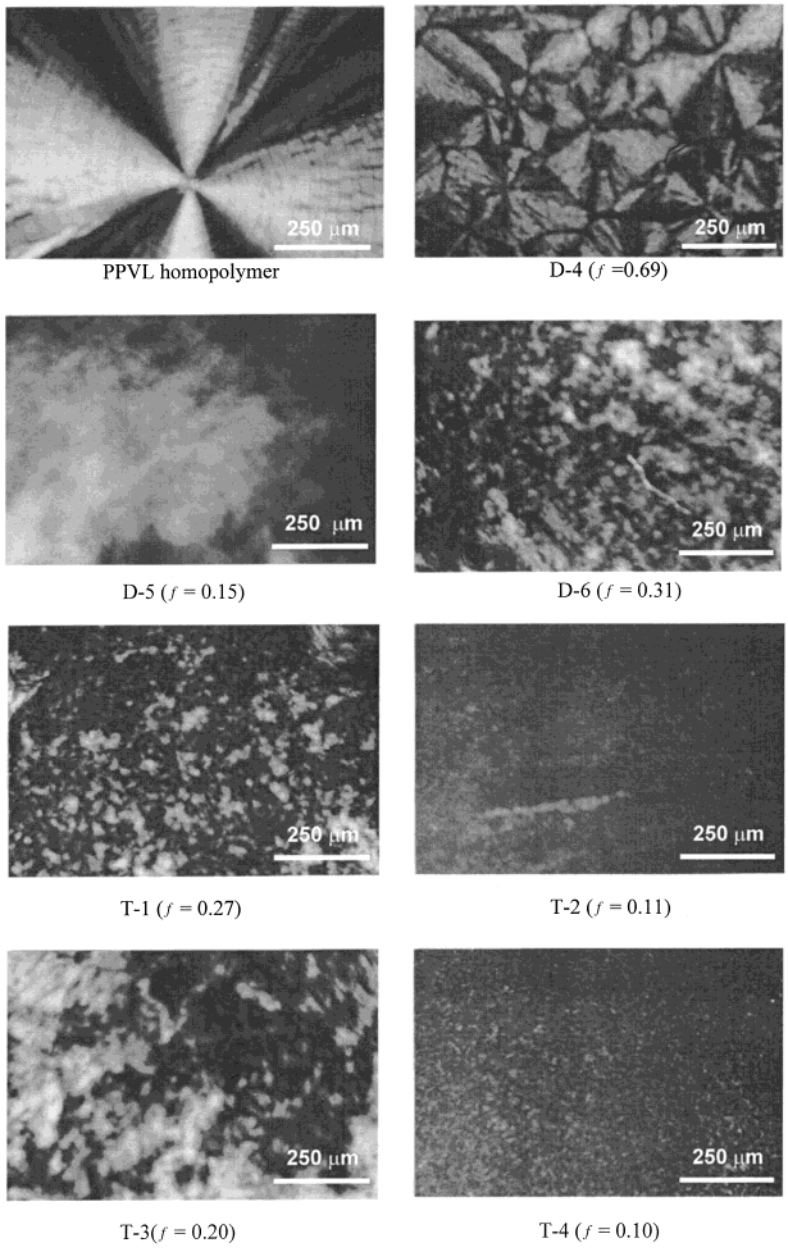

Figure 13. Polarized optical micrographs of each sample at T_c by cooling rate of 10 °C/min from the melt to T_c.

as the minor component ($f_{PPVL} \cong 0.10-0.31$). Since no spherulitic crystalline structures were observed after crystallization in the block copolymers with low f_{PPVL}, we can conclude that crystallization may not disrupt the preexisting morphology of these amorphous/crystalline block copolymers in the melt.

Conclusion

A new method was developed employing site transformation from living cationic to anionic ring-opening polymerization to prepare block copolymers with well-defined structural integrity containing rubbery PIB block and crystalline PPVL block. It was shown that PIB ω- and α,ω-carboxylate, obtained by living cationic polymerization of IB, followed by in situ capping with DPE, quenching with MTSP and hydrolysis of ω- and α,ω-methoxycarbonyl functionalized PIB, efficiently initiates the polymerization of PVL. High-temperature GPC, ^{1}H, and ^{13}C NMR spectroscopy indicated that poly(IB-*b*-PVL) and poly(PVL-*b*-IB-*b*-PVL) copolymers with various compositions and high structural integrity can be obtained by this method.

Crystallization behavior from the ordered melt was strongly dependent on the composition of these amorphous/crystalline di- and triblock copolymers. A drastic reduction of T_c was observed for block copolymers having spherical and cylindrical PPVL microstructures, implying homogeneous nucleation-controlled crystallization within PPVL microstructures. Further studies on crystallization and microstructural development using polarized optical microscopy confirmed that crystallization of PPVL segment was confined within spherical and cylindrical morphologies of block copolymers.

Acknowledgment. Financial support from National Science Foundation (DMR-9806418) is gratefully acknowledged. The authors are also grateful to P. Eiselt

and H.-C. Wang (Exxon Chemical Co.) for high-temperature GPC measurement and Z. Jedlinski and M. Kowalczuk for helpful comments.

References and Notes

(1) Förster, S.; Antonietti, M. *Adv. Mater.* **1998**, *10*, 195.
(2) Trzaska, S. T.; Lee, L.-B. W.; Register, R. A. *Macromolecules* **2000**, *33*, 9215.
(3) Mecerreyes, D.; Dubois, Ph.; Jérôme, R.; Hedrick, J. L.; Hawker, C. J. *J. Polym. Sci., Polym. Chem. Ed.* **1999**, *37*, 1923.
(4) Fujimoto, T.; Zhang, H.; Kazama, T.; Isono, Y.; Hasegawa, H.; Hashimoto, T. *Polymer* **1992**, *33*, 2208.
(5) (a) Gyor, M.; Fodor, Zs.; Wang, H.-C.; Faust, R. *J. Macromol. Sci., Pure Appl. Chem.* **1994**, *A31*, 2055. (b) Fodor, Zs.; Faust, R. *J. Macromol. Sci., Pure Appl. Chem.* **1996**, *A33*, 305.
(6) (a) Ryan, A. J.; Hamley, I. W.; Bras, W.; Bates, F. S. *Macromolecules* **1995**, *28*, 3860. (b) Hamley, I. W. *The Physics of Block Copolymers*; Oxford Univeristy Press: Oxford, 1998. (c) Nojima, S.; Tanaka, H.; Rhodi, A.; Sasaki, S. *Polymer* **1998**, *39*, 1727. (d) Quiram, D. J.; Register, R. A.; Marchand, G. R.; Adamson, D. H. *Macromolecules* **1998**, *31*, 4891. (e) Park, C.; De Rosa, C.; Fetters, L. J.; Thomas, E. L. *Macromolecules* **2000**, *33*, 7931. (f) Zhu, L.; Cheng, S. Z. D.; Calhoun, B. H.; Ge, Q.; Quirk, R. P.; Thomas, E. L.; Hsiao, B. S.; Yeh, F.; Lotz, B. *J. Am. Chem. Soc.* **2000**, *122*, 5957.
(7) Sipos, L.; Zsuga, M.; Deák, G. *Macromol. Rapid Commun.* **1995**, *16*, 935.
(8) Storey, R. F.; Sherman, J. W.; Brister, L. B. *Polym. Prepr. (Am. Chem. Soc., Div. Polym. Chem.)* **2000**, *41* (1), 690.
(9) Fodor, Zs.; Hadjikyriacou, S.; Li, D.; Faust, R. *Polym. Prepr.* **1994**, *35* (2), 492.
(10) Hadjikyriacou, S.; Fodor, Zs.; Faust, R. *J. Macromol. Sci., Pure Appl. Chem.* **1995**, *A32* (6), 1137.
(11) Hadjikyriacou, S.; Faust, R. *ACS Polym. Mater. Sci. Eng.* **1997**, *76*, 300.
(12) Koroskenyi, B.; Faust, R. *ACS Symp. Ser.* **1998**, *704*, 135.
(13) Harris, J. F., Jr.; Sharkey, W. H. *Macromolecules* **1986**, *19*, 2903.
(14) Jedlinski, Z.; Kurcok, P.; Matuszowicz, M.; Matuszowicz, A.; Dubois, P.; Jérôme, R.; Kricheldorf, H. R. *Macromolecules* **1995**, *28*, 7276.
(15) Jedlinski, Z.; Kurcok, P.; Matuszowicz, A.; Dubois, P.; Jérôme, R.; Kricheldorf, H. R. *Macromol. Rapid Commun.* **1995**, *16*, 513.
(16) Kurcok, P.; Kowalczuk, M.; Jedlinski, Z. *Macromolecules* **1994**, *27*, 4833.
(17) Kurcok, P.; Kowalczuk, M.; Hennek, K.; Jedlinski, Z. *Macromolecules* **1992**, *25*, 2017.
(18) Koroskenyi, B.; Faust, R. *ACS Symp. Ser.* **1998**, *704*, 135.
(19) Lorenz, C. E. U.S. Patent 3 291 810 (Dec 13, 1966, to DuPont).
(20) Anisworth, C.; Chen, F.; Kuo, Y. *J. Organomet. Chem.* **1972**, *46*, 59.
(21) Whitmore, F. C.; Wilson, C. D.; Capinjola, J. V.; Tonberg, C. O.; Fleming, G. H.; McGrew, R. V.; Cosby, J. N. *J. Am. Chem. Soc.* **1941**, *63*, 2035.
(22) Györ, M.; Wang, H.-C.; Faust, R. *J. Macromol. Sci., Pure Appl. Chem.* **1992**, *A29*, 639.
(23) Kwon, Y.; Faust, R. *Polym. Prepr. (Am. Chem. Soc., Div. Polym. Chem.)* **2000**, *41* (2), 1597.
(24) Kwon, Y.; Faust, R.; Chen, C. X.; Thomas, E. L. *Polym. Mater. Sci. Eng.* **2001**, *84*, 843.
(25) Scandola, M.; Focarete, M. L.; Gazzano, M.; Matuszowicz, A.; Sikorska, W.; Adamus, G.; Kurcok, P.; Kowalczuk, M.; Jedlinski, Z. *Macromolecules* **1997**, *30*, 7743.
(26) Noah, J.: Prud'homme, R. E. *Macromolecules* **1979**, *12*, 300.
(27) Duchesne, D.; Prud'homme, R. E. *Polymer* **1979**, *20*, 1199.
(28) Quiram, D. J.; Register, R. A.; Marchand, G. R. *Macromolecules* **1997**, *30*, 4551.
(29) (a) Weimann, P. A.; Hajduk, D. A.; Chu, C.; Chaffin, K. A.; Brodil, J. C.; Bates, F. S. *J. Polym. Sci., Polym. Phys. Ed.* **1999**, *37*, 2053. (b) Zhu, L.; Cheng, S. Z. D.; Calhoun, B. H.; Ge, Q.; Quirk, R. P.; Thomas, E. L.; Hsiao, B. S.; Yeh, F. *J. Am. Chem. Soc.* **2000**, *122*, 5957.
(30) Chen, H.-L.; Hsiao, S.-C.; Lin, T.-L.; Yamauchi, K.; Hasegawa, H.; Hashimoto, T. *Macromolecules* **2001**, *34*, 671.
(31) Konrad, M.; Knoll, A.; Krausch, G.; Magerle, R. *Macromolecules* **2000**, *33*, 5518.
(32) Meille, S. V.; Konishi, T.; Geil, P. H. *Polymer* **1984**, *25*, 773.

MA011739B